Research Article

Cancer Prevention Research

The Effect of Mouse Strain, Sex, and Carcinogen Dose on Toxicity and the Development of Lung Dysplasia and Squamous Cell Carcinomas in Mice

Laura Riolobos[1], Ekram A. Gad[1], Piper M. Treuting[2], Andrew E. Timms[3], Elliot A. Hershberg[1], Lauren R. Corulli[1], Erin Rodmaker[1], and Mary L. Disis[1]

Abstract

In order to translate new treatments to the clinic, it is necessary to use animal models that closely recapitulate human disease. Lung cancer develops after extended exposure to carcinogens. It has one of the highest mutation rates of all cancer and is highly heterogenic. Topical treatment with N-nitrosotris-(2-chloroethyl) urea (NTCU) induces lung squamous cell carcinoma (SCC) with nonsynonymous mutation rates similar to those reported for human non–small cell lung cancer. However, NTCU induces lung cancer with variable efficacy and toxicity depending on the mouse strain. A detailed characterization of the NTCU model is needed. We have compared the effect of three different NTCU doses (20, 30, and 40 mmol/L) in female and male of NIH Swiss, Black Swiss, and FVB mice on tumor incidence, survival, and toxicity. The main findings in this study are (1) NIH Swiss mice present with a higher incidence of SCC and lower mortality compared with Black Swiss and FVB mice; (2) 30 mmol/L NTCU dose induces SCC at the same rate and incidence as the 40 mmol/L dose with lower mortality; (3) female mice present higher grade and incidence of preinvasive lesions and SCC compared with males; (4) NTCU-induced transformation is principally within the respiratory system; and (5) NTCU treatment does not affect the ability to elicit a specific adaptive immune response. This study provides a reference point for experimental designs to evaluate either preventive or therapeutic treatments for lung SCC, including immunotherapies, before initiating human clinical trials.

Introduction

Preclinical rodent models for cancer have not replicated human studies due in part to their inability to accurately recapitulate the complexity of human cancer. Lung cancer develops after an extended exposure to carcinogens. It has one of the highest mutation rates of all cancer and is highly heterogenic. Transgenic lung cancer models, such as the *KrasG12D p53*$^{-/-}$ for adenocarcinoma or the *Lkb1* knockout models for squamous cell carcinoma (SCC), do not represent the heterogeneity, mutational burden, and genomic landscape found in human lung cancer (1). In addition, for the study of immunotherapy, they do not recapitulate the tumor microenvironment observed in humans (2). Syngeneic implanted tumors grow too fast *in vivo* to elicit adaptive immune responses, do not develop significant immune-suppressive elements, and have lower tumor-infiltrating lymphocytes (TIL) than spontaneous tumors (3). Moreover, both the syngeneic implant tumors and the genetically engineered mouse (GEM) models lack the early preinvasive events in lung cancer oncogenesis, and therefore, they are not ideal for chemoprevention studies (4).

Chemically induced tumors are often used to study lung cancer therapies. Tumors in these models present with a higher mutational load, significant heterogeneity, and slower tumor growth rates than GEM and tumor implant models. Yet chemically induced lung tumors have not been well characterized, especially regarding the kinetics of tumor growth and chemical treatment-related toxicity. Topical treatment with N-nitrosotris-(2-chloroethyl)urea (NTCU) induces lung SCC in mouse with variable efficacy depending on the strain (5, 6). N-nitroso compounds, such

[1]UW Medicine Cancer Vaccine Institute, University of Washington, Seattle, Washington. [2]Department of Comparative Medicine, University of Washington, Seattle, Washington. [3]Center for Developmental Biology and Regenerative Medicine, Seattle Children's Research Institute, Seattle, Washington.

Note: Supplementary data for this article are available at Cancer Prevention Research Online (http://cancerprevres.aacrjournals.org/).

Corresponding Author: Laura Riolobos, University of Washington, 850 Republican St., Box 358050, Seattle, WA 98109. Phone: 206-221-6454; Fax: 206-685-3128; E-mail: lriolobo@uw.edu

Cancer Prev Res 2019;12:507–16

doi: 10.1158/1940-6207.CAPR-18-0442

as NTCU, are nicotine-derived compounds present in tobacco, which are transformed within the body to alkylating agents that attack DNA (7). Mice treated with NTCU develop bronchial epithelia dysplasia and metaplasia that progress to invasive SCC similarly to the development of human lung SCC. Exome sequencing of cell lines and tumors derived from the NTCU model has shown nonsynonymous mutation rates comparable with those reported for human non–small cell lung cancer (8, 9). However, induction of lung SCC with NTCU severely reduces survival of treated animals, with mortality rates of 32% to 55% occurring before the development of tumors (10, 11). There are no reported studies showing an NTCU dose titration to analyze the effect of mid-range doses on toxicity, survival, and induction of lung SCC. This model has been extensively used for prevention studies, and improved model characterization is necessary to evaluate the success of chemopreventive agents. In addition, although sex effect on cancer susceptibility has been reported, it has not been studied if sex influences the development of SCC induced by NTCU in multiple strains of mice (12).

We questioned if lower doses of NTCU could still induce SCC while preventing chemical-associated toxicity. We have compared the effect of three different doses of NTCU (20, 30, and 40 mmol/L) in female and male NIH Swiss, Black Swiss, and FVB mice. For each sex, NTCU dose, and strain, we have assessed: (1) mouse weight and survival; (2) incidence and grade of hyperplasia, dysplasia, and SCC; and (3) other respiratory tract and off-target lesions caused by NTCU. Finally, for the study of immune therapy, it is critical to evaluate whether treatment with NTCU influences the ability to generate an immune response.

Materials and Methods

Mouse lung cancer models

FVB mice (FVB/NJ, Stock No. 001800) were purchased from the Jackson Laboratory. NIH Swiss (NIH(S)-550) and Black Swiss (NIHBL(S)-492) mice were purchased from Charles River Laboratory. Mice were housed in a specific pathogen-free facility (details in the Supplementary Methods). At 5 to 9 weeks of age, animals were randomized to the different treatment groups. Six to 10 mice were included for untreated and acetone-treated control groups, and 12 to 16 mice were studied for each of the NTCU-treated groups. Male and female mice were distributed at 50% in every group. NTCU (Toronto Research Chemicals Inc.) was dissolved in acetone. Forty-eight hours before treatment, the dorsal skin was shaved, and acetone or NTCU at the appropriate concentration was applied every 3 days in 25 μL drops for 32 weeks. Animals were monitored twice a week for weight loss and health concerns such as labored respiration, disheveled appearance, decreased activity, and anorexia. All the procedures were approved by the University of Washington Institutional Animal Care and Use Committee.

Histologic evaluation of toxicity and lung neoplasia

One animal from untreated and acetone groups and two animals, one female and one male, from the NTCU groups were sacrificed at 8, 16, and 24 weeks after initiation of treatment. The remaining mice in each group were sacrificed at 32 weeks. Mice were euthanized by overdose with isoflurane and cervical dislocation followed by complete necropsy. The following samples were collected for histological analysis: lungs, skin from application site, stomach, kidney, liver and head (including brain, ear canal, and oral and nasal cavities) were collected for histologic analysis. Lungs were removed, weighed, and inflated with 10% neutral buffered formalin. All tissues were immersed fixed in 10% formalin. Samples were processed routinely, embedded in paraffin, stained with hematoxylin and eosin (H&E), and examined by a board-certified veterinary pathologist (P.M. Treuting) for evidence of neoplasia, nonneoplastic lesions, and toxicity. Two serial sections, 4–6 μm thick, were analyzed for each tissue and animal. Lung proliferative and neoplastic grading was carried out under bright field microscopy on H&E samples using criteria previously described (6, 11, 13, 14). Images were captured using a Nikon Eclipse 80i with a Nikon Digital Sight DS-Fi1 camera and processed (global white balance and contrast) and plated with Adobe Photoshop 2015. Slides were scanned using Hamamatsu NanoZoomer S60 (Hamamatsu Photonics K.K.). Percentage of tumor area for each mouse was manually selected and quantified using QuPath (15).

Immunohistochemistry

The following antibodies were used: anti-CD4 (eBioscience, clone 4SM95), anti-CD8 (eBioscience, clone 4SM15), and anti–PD-L1 (Cell Signaling Technology, clone D5V3B). Full details about IHC staining protocols are provided in the Supplementary Methods. Nine NTCU-treated NIH Swiss mice (5 female and 4 male) presenting tumors were used for quantification. Two to three representative areas containing SCC were randomly selected, and the number of $CD4^+$ and $CD8^+$ cells was quantified using QuPath (15). For PD-L1, three representative tumor areas with the highest number of PD-L1–positive cells were used for quantification. Percentage of positive cells was corrected for the total number of SCC cells in the counted area.

Evaluation of adaptive immune response

FVB or NIH Swiss mice, female, five animals per group, were vaccinated 4 times every 10 days with an IGF1R vaccine containing three peptides (100 μg/each): IGF1R p1166-1182, IGF1R p1212-1226, and IGF1R p1302-1325 (16). Mice received a fifth booster vaccine 15 days before sacrifice. NTCU (40 mmol/L) was applied twice a

week for a total of 4 weeks, before or concomitant to vaccination. Spleens were processed according to our previously published methods, and the immune response to vaccinated antigen was analyzed by IFNγ ELISPOT assays as published (17). Antigens tested included the IGF1R peptide pool contained in the vaccine (10 μg/mL each peptide), HIVp17 (ERFALNPGLLETSEGCK, 10 μg/mL), and concanavalin A (ConA, 2.5 μg/mL). Data are reported as corrected spots per well (CSPW, mean number of spots for each experimental antigen minus the mean number of spots detected in no-antigen control wells).

Immune phenotype evaluation by flow cytometry

Antibodies and reagents used for flow cytometry are listed in the Supplementary Methods. Cells were acquired using FACSCanto flow cytometer (BD Biosciences) and analyzed using FlowJo software (Tree Star Inc.). Results are reported as the mean ± SD of the total percentage of each cell population as indicated.

RNA sequencing

Five NIH Swiss mice presenting lung SCC and 5 control healthy mice were used for laser capture microdissection (LCM). Microdissection was performed in a LMD7000 microscope (Leica Microsystems GmbH). Full details about the protocol are provided in the Supplementary Methods. RNA was extracted using the RNeasy FFPE kit (Qiagen), and libraries were prepared from using the SMARTer Stranded Total RNA-Seq Kit – Pico Input Mammalian (Clontech Laboratories, Inc.). Sequencing was performed using an Illumina HiSeq 2500 generating 50 base-pair paired-end reads. Reads of low quality were filtered, and adapters trimmed using Cutadapt v1.9.1. Alignment to the reference genome (UCSC mm10) was performed using TopHat v2.0.1, and RNA counts were generated for each gene using the Python package HTSeq v0.6.1, employing the "intersection-strict" overlap mode. DESeq2 (18) was used to normalize and transform the data, to examine the relationship between samples (by plotting the first two principal components), and to test for differential expression. Data derived from the RNA sequencing have been deposited in GEO (https://www.ncbi.nlm.nih.gov/geo/), accession number (pending). Three human microarray datasets were analyzed using the web-based GEO2R (https://www.ncbi.nlm.nih.gov/geo/geo2r/). The most significantly differentially expressed genes were converted to their mouse counterpart using HCOP (https://www.genenames.org/tools/hcop/).

Statistical analysis

Graphs and ANOVA comparisons were completed using GraphPad Prism v7 software. A one-way ANOVA with Tukey posttest was used for comparison of one variable between the different treatment groups, and a two-way ANOVA with Bonferroni or Tukey posttest was used for grouped comparisons with more than one variable. Unless reported separately, there were no sex differences noted by two-way ANOVA with Bonferroni correction test, and therefore sexes were combined for analysis. Kaplan–Meier curves were generated to show overall survival. The log-rank (Mantel–Cox) test was used for survival curves comparison. Note that χ^2, with a confidence interval (CI) of 95%, was used to compare proportions in survival for each mouse strain treated with NTCU. Linear regression was used to evaluate the relation between lung weight and disease burden. Significance was considered at $P < 0.05$ for statistical tests, except for the survival curves comparison. Survival curves–corrected P value was 0.0083.

Results

Animals treated with NTCU lose weight in a dose-dependent manner

Mice treated with 20 mmol/L NTCU lose less weight compared with the 30 and 40 mmol/L groups. For each analyzed mouse strain, weight loss in the 20 mmol/L group was significantly lower than the 40 mmol/L treatment group (20 vs. 40 mmol/L, $P < 0.0001$), and not significantly different from the acetone control group (Supplementary Table S1). Weight loss in the 30 mmol/L group was dependent on strain. For the NIH Swiss mice, weight change in mice treated with 30 mmol/L was not significantly different from the 40 mmol/L NTCU group (Fig. 1A; Supplementary Table S1). For the Black Swiss, mice weight loss in the 30 mmol/L group was significantly lower than the 40 mmol/L treatment group ($P = 0.0189$; Fig. 1B). FVB mice show no differences in weight change between the 30 mmol/L and the 40 mmol/L groups (Fig. 1C). No significant differences were observed between the untreated control group and the acetone group in any mouse strain. Comparison of weight loss between females and males was not significantly different for any of the strains or NTCU doses assayed (Supplementary Table S2), and data from males and females were combined for analysis.

Survival of mice treated with NTCU is dose- and strain-dependent

NIH Swiss and Black Swiss mice treated with 20 and 30 mmol/L NTCU showed significantly lower mortality compared with the standard 40 mmol/L NTCU dose (NIH Swiss: 20 vs. 40 mmol/L, $P < 0.0001$; 30 vs. 40 mmol/L, $P = 0.0004$; Black Swiss: 20 vs. 40 mmol/L, $P < 0.0001$; 30 vs. 40 mmol/L, $P < 0.0025$; Fig. 1D and E). For the FVB mice, survival rates of the three NTCU-treatment groups do not significantly differ from each other (20 vs. 40 mmol/L, $P = 0.0288$; 20 vs. 30 mmol/L, $P = 0.0326$; 30 vs. 40 mmol/L, $P = 0.6364$; Fig. 1F).

The mean of survival days in the NIH Swiss mice for each treatment group was 20 mmol/L NTCU 219 ± 40 (95% CI, 191–248), 30 mmol/L NTCU 187 ± 37 (95% CI,

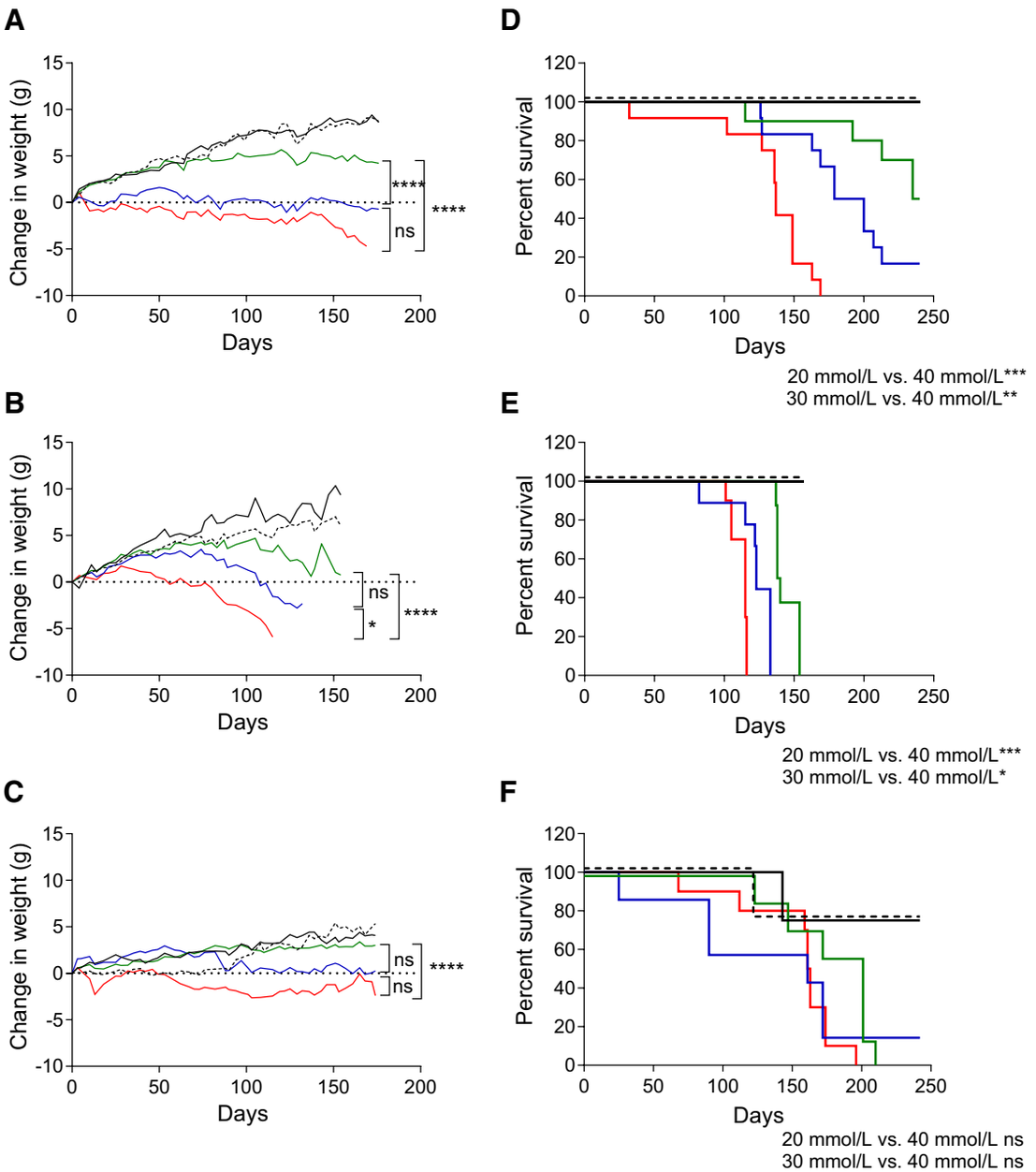

Figure 1.

Dose of NTCU correlates with animal weight loss and mortality of treated animals. NIH Swiss (**A** and **D**), Black Swiss (**B** and **E**), and FVB mice (**C** and **F**) untreated (black line) or treated with acetone (black dotted), 20 mmol/L NTCU (green), 30 mmol/L NTCU (blue), or 40 mmol/L NTCU (red). Change in animal weight calculated as the difference between weight at a certain time point and the weight at day 0 of treatment. Weight graphs: *, $P < 0.05$; **, $P < 0.01$; ***, $P < 0.001$; and ****, $P < 0.0001$. Healthy animals euthanized at intermediate time-points for analysis have not been included in the survival curve. Survival curves–corrected P value is 0.0083 (*, $P < 0.0083$; **, $P < 0.0008$; and ***, $P < 0.0001$).

163–210), and 40 mmol/L NTCU 132 ± 36 (95% CI, 109–155). The mean of survival for the Black Swiss mice was: 20 mmol/L NTCU 144 ± 8 (95% CI, 137–151), 30 mmol/L NTCU 122 ± 16 (95% CI, 109–134), and 40 mmol/L NTCU 112 ± 6 (95% CI, 108–116). The mean of survival days for the FVB strain was: 20 mmol/L NTCU 179 ± 33 (95% CI, 149–210), 30 mmol/L NTCU 136 ± 72 (95% CI, 70–203), and 40 mmol/L NTCU 161 ± 22 (95% CI, 144–178). Mean survival was not reached in the untreated and acetone groups, and no differences in survival were found between them. In the FVB cohort, 2 female mice died in the control groups, one in the untreated group and one in the acetone group. Unfortunately, we were not able to perform necropsy in these mice,

and the cause of death remains unknown. We cannot exclude that some of the mice that died in NTCU groups were unrelated to the treatment or to the development of lung disease.

A significant interaction between mortality and strain was found. For any NTCU treatment group, Black Swiss and FVB were more likely to die than NIH Swiss mice. There is a 91.7% ($n = 36$) probability of dying in Black Swiss, 47.2% ($n = 36$) in FVB, and 43.5% ($n = 46$) in NIH Swiss mice treated with NTCU [χ^2 (2, $n = 118$) = 22.58, $P < 0.0001$)]. Comparison of mean of survival between female and male mice was not significant for any of the strains and NTCU doses assayed (Supplementary Table S3). Data from male and female mice have been combined for analysis.

Development and grade of preinvasive lesions, hyperplasia, and dysplasia depend on NTCU dose, sex, and mouse strain

Hyperplasia and dysplasia were observed earlier in Black Swiss and NIH Swiss mice treated with NTCU compared with FVB. Hyperplasia was present at 8 weeks after NTCU treatment for all the strains, with grade increasing at higher NTCU doses. Minimal–mild squamous and adenomatous atypical dysplasia was observed after 8 weeks of treatment for the NIH Swiss and Black Swiss, and at 16 weeks for the FVB. High-grade hyperplasia, squamous metaplasia, and high-grade dysplasia were found at 16 weeks in the Black Swiss mice, and at 24 weeks for the NIH Swiss and FVB mice.

Females presented with a higher degree (moderate–severe versus minimal–mild) squamous metaplasia and dysplasia compared with male. In the NIH Swiss strain, high-grade metaplasia was present in 80% of females versus 17% of males in the 20 mmol/L NTCU group, and 60% of females versus 50% of males in the 30 mmol/L group. No difference between females and males was observed in the 40 mmol/L dose. For FVB mice, high-grade squamous metaplasia was found in 25% of females versus 0% of males in the 30 mmol/L group, and 60% of females versus 33% of males in the 40 mmol/L cohort.

NTCU-induced SCC develops at the same incidence and rate in the 30 mmol/L and 40 mmol/L NTCU doses and shows a gene expression profile comparable with human SCC

In NIH Swiss and FVB mice, SCCs are present after 24 weeks of NTCU treatment in the 30 mmol/L and 40 mmol/L NTCU groups. NIH Swiss mice treated with 20 mmol/L NTCU developed invasive SCC after 32 weeks of NTCU treatment, whereas SCCs were not present in the FVB mice treated with the 20 mmol/L dose. The percentage of mice treated with NTCU for 24 to 32 weeks presenting SCC in the 20, 30, and 40 NTCU groups was: (1) NIH Swiss: 36%, 60%, and 57%; and (2) FVB: 0%, 20%, and 25%. Only 2 mice from the Black Swiss strain treated with 30 mmol/L NTCU developed small SCC at 16 weeks, and no tumors were observed for the 20 and 40 mmol/L doses at any time point. In addition to the higher percentage of mice found with tumors in the NIH Swiss mice, this strain presented with the largest tumors (>5 mm) as compared with FVB mice. Female NIH Swiss presented with the largest SCC (>5 mm) as compared with male. No SCCs were found in the untreated or acetone-treated control animals.

Total gene expression of normal lung and SCC from NIH Swiss mice was determined by RNA sequencing and compared with three independent public human datasets. Mouse expression data were consistent with genes up- and downregulated in the human data. The analysis of the top 150 genes upregulated in the human datasets showed they were also upregulated in the mouse SCC, whereas the top 150 genes downregulated in the human data were downregulated in mouse (Supplementary Fig. S1).

In addition to lung SCC, there was one example of adenosquamous carcinoma with a central adenomatous foci and peripheral squamous cell differentiation in the NIH Swiss 30 mmol/L NTCU group as previously described (19). Spontaneous adenomas/adenocarcinomas without squamous differentiation were also observed at low frequency (3%) in all the groups of the FVB strain, as previously described, and have not been included in the analysis (11, 13).

NTCU induces inflammation and damage of upper and lower respiratory tract epithelium with variable incidence depending on mouse strain

In addition to lung SCC, NTCU induced preneoplastic changes in the nasal and trachea epithelia and was associated with nonneoplastic lesions in the lung, such as peribronchiolar fibrosis, inflammation, foamy macrophage accumulations, and pneumonia. Incidence of other respiratory tract and off-target lesions on NTCU-treated animals is summarized in Table 1. Neutrophilic exudative rhinitis and sinusitis were found in the three mouse strains examined, being more frequent in the Black Swiss mice (70%) compared with the NIH Swiss and FVB (28% and 9%, respectively). In the Black Swiss strain, rhinitis and sinusitis were frequently accompanied by nasal epithelia erosions with hyperplasia and metaplasia. Trachea epithelia developed hyperplasia and dysplasia in the three mouse strains assayed with similar incidence (97% of NIH Swiss, 88% of Black Swiss, and 82% of FVB). Nonneoplastic lesions were present in the lungs and included pneumonia and peribronchiolar fibrosis, typically accompanied by loss of respiratory epithelium and lymphoid aggregates (Supplementary Fig. S2). Pneumonic lesions varied from acute neutrophilic to histiocytic to organizing with fibrosis. The highest incidence of pneumonia occurred in the Black

Table 1. Incidence of respiratory tract and off-target lesions on NTCU-treated animals; percentage of animals with the indicated lesions is shown

	NIH Swiss		Black Swiss		FVB	
	Acetone	NTCU	Acetone	NTCU	Acetone	NTCU
Respiratory tract						
Nasal cavity						
Hyperplasia/metaplasia	0	0	0	13	0	0
Rhinitis/sinusitis	0	28	0	70	0	9
Trachea hyperplasia/dysplasia	0	97	0	88	0	82
Lung						
Peribronchiolar fibrosis	0	37	0	47	0	18
Lymphoid aggregates	0	17	0	33	0	12
Pneumonia	0	7	0	73	0	9
Off target effects						
Dermatitis at application site	0	83	25	67	0	19
Ear auricular dermatitis	0	15	0	0	0	0
Hyperplastic accessory sex glands	0	0	0	17	0	58

Swiss group, with 73% of the mice developing pneumonia. Black Swiss mice from the three NTCU doses prematurely died between 77 and 154 days of treatment, probably due to the development of NTCU-related rhinitis, sinusitis, and pneumonia. Lower incidence of pneumonia was present in NIH Swiss mice (7%) and FVB (9%). No differences were observed by sex.

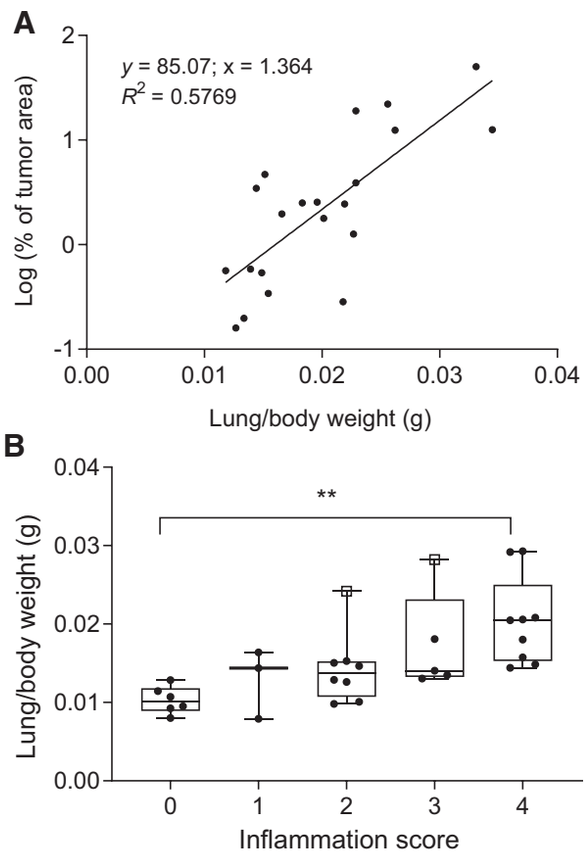

Figure 2.
Lung weight correlates with tumor burden determined by histology and inflammation grade. **A,** Percentage of tumor area measured in H&E sections related to lung weight in NIH Swiss mice. **B,** Lung weight of Black Swiss mice without pneumonia (grade 0) and mice with pneumonia classified by inflammation grade. No inflammation (0), minimal (1), mild (2), moderate (3), and severe (4). The two Black Swiss mice presenting tumors are shown as open squares.

The most common off-target effect of the NTCU was dermatitis at the application site for the three mouse strains studied. Ulcerative chronic proliferative dermatitis at the application site, frequently accompanied by dermal fibrosis, was found in 83% of NIH Swiss mice treated with NTCU and at lower frequency in Black Swiss (67%) and FVB (19%). NTCU-related severe ear auricular chondritis and dermatitis was present at low incidence (15%) exclusively in the NIH Swiss mice. There was no histologic evidence of neoplasia in the pinnae of three of the more severely affected. We also observed the development of perianal swelling in FVB and Black Swiss mice treated with NTCU, being more frequent in FVB mice (58%). Swelling occurred in both female and male with the same incidence. Histologic analysis of this region showed cystic hyperplastic sexual glands in the treated mice. One FVB mouse developed esophageal and gastric SCC. No signs of further NTCU-meditated toxicity or neoplasia were present in the other organs histologically examined.

Evaluation of tumor burden by lung weight is not specific for cancer due to the confounding pneumonia

Increase in lung weight was observed in NIH Swiss and Black Swiss mice treated with NTCU, but not in the FVB group. For the NIH Swiss mice, lung weight was significantly higher in mice treated with 30 mmol/L NTCU for 24 weeks (control 0.30 ± 0.03 g, 30 mmol/L NTCU 0.50 ± 0.09 g, $P = 0.0009$) and in mice treated with 20 and 30 mmol/L NTCU for 32 weeks (control group: 0.32 ± 0.04 g; 20 mmol/L NTCU: 0.42 ± 0.07 g, $P = 0.0023$; 30 mmol/L NTCU: 0.46 ± 0.07 g, $P = 0.0001$). In the Black Swiss cohort, lung weight was significantly higher in mice treated with 30 mmol/L NTCU for 16 weeks (30 mmol/L NTCU 0.48 ± 0.10 g vs. control 0.28 ± 0.05 g, $P = 0.043$), and in mice treated with 20 mmol/L NTCU for 24 weeks (20 mmol/L NTCU 0.58 ± 0.07 g vs. untreated and acetone control 0.32 ± 0.04 g, $P < 0.0001$). No significant differences

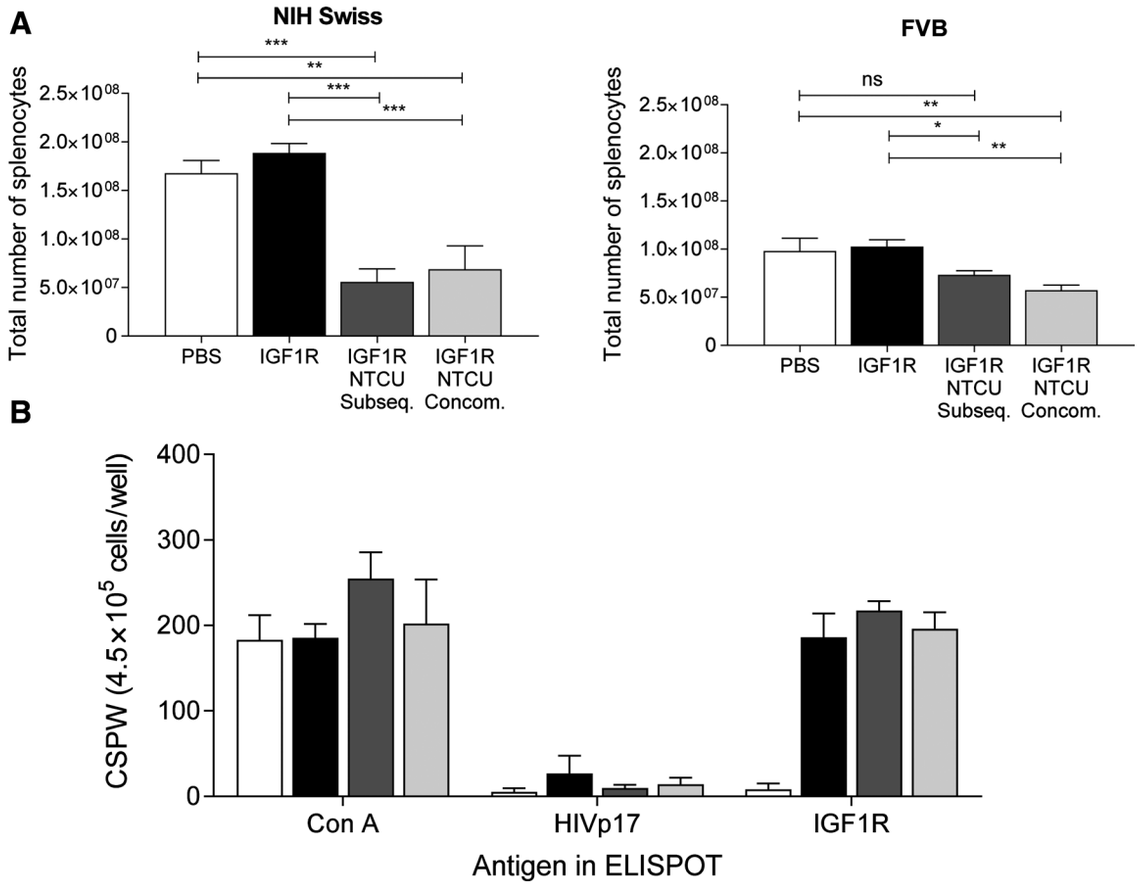

Figure 3.

Treatment with NTCU reduces spleen cellularity without affecting ability to mount a robust immune response. NIH Swiss (left) and FVB (right) mice vaccinated with PBS (white), IGF-IR (black), IGF-IR followed by NTCU treatment (dark gray), or IGF-IR concomitant with NTCU treatment (light gray). **A,** Total number of splenocytes. **B,** IFNγ ELISPOT conducted on splenocytes from vaccinated animals, five animals per group. Concanavalin A (Con A) was used as positive control, and HIV peptide (HIVp17) was used as nonspecific response control. CSPW, corrected spots per well. Mean and SEM are shown (*, $P < 0.05$; **, $P < 0.01$; ***, $P < 0.001$).

in lung weight were observed in the FVB mice between NTCU-treated and untreated groups. Tumor burden, calculated as the percentage of tumor area of the total lung area in histologic sections, showed correlation with lung weight only for the NIH Swiss cohort [$R^2 = 0.5769$, $F(1,19) = 25.91$, $P < 0.0001$; Fig. 2A). No correlation between lung weight and tumor burden was found for the FVB group [$R^2 = 0.0831$, $F(1,3) = 0.2720$, $P = 0.6381$]. For the Black Swiss mice, there were not enough data to study correlation between lung weight and tumor burden, as only 2 mice in this group develop SCC. However, Black Swiss mice developed NTCU-related pneumonia, and lung weight was significantly higher for those mice with moderate-to-severe pneumonia compared with those mice with no inflammation (mean ± SD; no inflammation 0.283 ± 0.05 g, minimal 0.329 ± 0.04 g, mild 0.377 ± 0.05 g, moderate 0.439 ± 0.11 g, and severe 0.542 ± 0.09 g; no inflammation vs. moderate $P = 0.0064$, no inflammation vs. severe $P < 0.0001$; Fig. 2B).

Treatment with NTCU reduces spleen cellularity without affecting ability to mount a robust immune response

The total number of splenocytes was lower in mice treated with 40 mmol/L NTCU for 4 weeks (Fig. 3A) compared with the untreated cohorts, although no change in viability was observed between the groups (Supplementary Table S4). Regardless of the decrease of cellularity in spleen, animals treated with NTCU demonstrated a robust and specific immune response similar to the vaccinated untreated group (Fig. 3B). Analysis of the different immune cell populations in splenocytes by flow cytometry showed a significant decrease in the regulatory myeloid-derived suppressor cell population (MDSC, $CD11b^+$ $Gr1^+$) in the NIH Swiss mice treated with NTCU simultaneously to vaccination ($P = 0.0024$), but not for the FVB mice (Supplementary Table S4). In addition, in NIH Swiss mice, the percentage of $CD8^+$ $PD\text{-}1^+$ T cells is lower in mice treated with NTCU either subsequently ($P = 0.0248$) or simultaneously ($P < 0.0001$) to vaccination. Percentage of $CD4^+$

PD-1$^+$ T cells is also lower in NIH Swiss mice treated with NTCU concomitantly to vaccination ($P = 0.0406$). No changes in PD-1 expression were observed in FVB mice. Percentage of CD3$^+$, CD4$^+$, CD8$^+$ T cells, and CD4$^+$FoxP3$^+$ T regulatory cells (Treg) did not change in the different treatment groups.

The effect of long-term treatment with NTCU on the immune system was evaluated in mice untreated or treated with 20 or 30 mmol/L NTCU for 24 to 32 weeks. NIH Swiss mice treated with 30 mmol/L NTCU showed a moderate but significant higher percentage of CD4$^+$ FoxP3$^+$ Tregs compared with the untreated and acetone-treated groups ($P = 0.01$, Supplementary Table S5). There were no significant changes in the percentage of CD3$^+$, CD4$^+$, CD8$^+$ T cells, or MDSC cells (Supplementary Table S5). In addition, no differences in the percentage of PD-1–expressing CD4$^+$ and CD8$^+$ T cells were observed between the different treatment groups.

NIH Swiss mice treated with NTCU presented CD4$^+$ and CD8$^+$ T cells accumulated in lymphoid aggregates close to main bronchi and around blood vessels, and were also present in the lung tissue surrounding the tumor (Supplementary Fig. S3). However, percentages of CD4$^+$ and CD8$^+$ T cells within the tumor were low (<5%), and there were not significant differences between female and male mice (female vs. male % of CD4$^+$ $P = 0.9731$, % of CD8$^+$ $P = 0.9913$). PD-L1 expression was heterogeneous within the tumor and between mice, and there was no significant difference between female and male ($P = 0.0730$). At an arbitrary cutoff of 1% for PD-L1 expression, 67% of the mice were PD-L1 positive.

Discussion

The main findings in this study are: (1) NIH Swiss mice present with a higher incidence of SCC and lower mortality and toxicity compared with Black Swiss and FVB mice; (2) 30 mmol/L NTCU dose induces SCC at the same rate and incidence than the 40 mmol/L dose with lower toxicity and mortality in treated mice; (3) female mice present higher grade and incidence of preinvasive lesions and SCC compared with male; (4) NTCU-induced transformation is principally within the respiratory system; and (5) NTCU treatment does not affect the ability to elicit a specific adaptive immune response in FVB and NIH Swiss strains.

Variation in mouse strain vulnerability to cancer has been previously reported in the literature (20–22). Wang and colleagues studied the mouse strain susceptibility to lung cancer after treatment with 40 mmol/L NTCU and classified the strains as resistant, intermediate, or susceptible to NTCU lung carcinogenesis (5). The study included C57BL/6N (resistant, no SCC), FVB (intermediate, SCC incidence 44%), and NIH Swiss mice (susceptible, SCC incidence 83%) among others. In addition to NIH Swiss and FVB mice, we have included Black Swiss strain, which has not been previously evaluated in the NTCU lung cancer model. Our study confirms the previously reported susceptibility for NIH Swiss and FVB (5, 11). Confounding pneumonia together with the low incidence of SCC in Black Swiss mice dissuades the use of this strain for this model. NIH Swiss presented with a higher incidence of SCC and lower mortality as compared with FVB. Therefore, we proposed that NIH Swiss mice should be used for those studies where endpoint is prevention or treatment of SCC.

Treatment with 40 mmol/L NTCU twice a week has been the standard to induce SCC in mice, yet this dose severely reduces survival of mice (10, 11). Hudish and colleagues showed that doses of 4 and 10 mmol/L in FVB mice are better tolerated, although do not induce dysplasia nor SCC. Here, we show that decreasing concentration of NTCU to 20 or 30 mmol/L improves mouse health and reduces mortality associated with treatment, while still inducing high-grade dysplasia and SCC. Furthermore, treatment with 30 mmol/L NTCU results in development of dysplasia and SCC at the same rate and incidence as the 40 mmol/L dose. Therefore, we suggest standardizing the 30 mmol/L NTCU dose for those studies evaluating treatments for SCC or prevention of progression from dysplasia to SCC. Treatment with 20 mmol/L NTCU can also be useful for prevention studies, as the disease progresses slowly at this dose, giving more time for the preventive agents to work.

This is the first study evaluating NTCU toxicity in multiple organs. NTCU induces chronic inflammation and transformation of respiratory epithelium. Dysplasia was observed in the trachea epithelia for all the strains evaluated, as previously described for FVB (23). Extensive NTCU-induced pneumonia was present in Black Swiss mice. Other NTCU-related lesions included ear auricular chondritis, dermatitis, and cystic changes in the accessory sex glands. One FVB mouse developed esophageal and gastric SCC, which is likely related to NTCU exposure, as these are extremely rare spontaneous tumors in the FVB strain. No signs of further NTCU-meditated toxicity or neoplasia were present in the other organs histologically examined in any of the mouse strains.

Sex is an important factor in cancer incidence, prognosis, and outcome (24–26). There are also significant sex differences in the prevalence and grade of respiratory diseases and lung cancer (27–29). Women are more susceptible to tobacco carcinogens and present increased risk for lung cancer development compared with men when adjusting for age and smoking history (30–32). In addition, females develop lung cancer at a younger age, even with less cigarettes consumed than males (25, 33). However, *in vivo* studies exploring cancer therapies in both sexes are rare. There is only one study for the NTCU lung cancer model that included female and male FVB mice, and the authors reported that females have greater dysplasia per area of lung compared with males (11). We have shown that for every strain studied, females present higher-grade

dysplasia, higher SCC incidence, and larger SCC lesions compared with males. Female C57BL/6 mice have greater numbers of type 2 inflammation cells in the lungs (34), and sex hormones contribute to lung inflammation and modulate the PD-1/PD-L1 pathway (35, 36). In order to account for this sex-based heterogeneity in tumor development and treatment responses, both female and male animals should be included in the evaluation of lung cancer therapies.

The percentage of $CD4^+$ and $CD8^+$ T cells as well as PD-L1 expression was heterogeneous within the tumor. Heterogeneity in TILs and PD-L1 expression has also been reported in human non–small cell lung cancer (37–39). Percentage of T cells in the mouse model was similar to the percentages observed in human non–small cell lung cancer (<5% TILs in >70% of patients; ref. 38). At a cutoff of 1% for PD-L1 expression, 48% of human lung SCC are PD-$L1^+$ (39), which is comparable with the 67% PD-$L1^+$ SCC observed in the mouse model.

Finally, we found that NTCU treatment reduces the total number of splenocytes in a dose-dependent manner. However, reduced cellularity does not affect the ability to mount a robust and specific T-cell response. In addition, we did not find increase in the expression of checkpoint inhibitors (PD-1) in the splenocytes of mice treated with NTCU, although there was a modest increase of $CD4^+$ Tregs in NIH Swiss mice treated with higher doses of NTCU. Therefore, NTCU does not have immunosuppressive effects, and we believe that this chemically induced lung cancer model is appropriate for evaluation of immunotherapies.

The NTCU SCC mouse model has several properties that resemble human lung cancer: heterogeneity of tumors, increased mutation burden, slow progression, and presence of premalignant lesions that evolve to invasive SCC similarly to the disease in lung cancer patients. Characterization of chemically induced tumor models is necessary to understand their advantages and limitations. This study provides a reference point for experimental designs to evaluate either preventive or therapeutic treatments for lung SCC, including immunotherapies, before initiating human clinical trials.

Disclosure of Potential Conflicts of Interest

M.L. Disis reports receiving commercial research grant from EMD Serono, Celgene, Seattle Genetics, Silverback Therapeutics, Pfizer, Janssen, and Epithany; has an ownership interest (including stock, patents, etc.) in Epithany; and has an expert testimony in Patent Royalties, U Washington. No potential conflicts of interest were disclosed by the other authors.

Authors' Contributions

Conception and design: L. Riolobos, M.L. Disis
Development of methodology: L. Riolobos, E.A. Gad, E.A. Hershberg, E. Rodmaker, M.L. Disis
Acquisition of data (provided animals, acquired and managed patients, provided facilities, etc.): L. Riolobos, P.M. Treuting, L.R. Corulli, E. Rodmaker
Analysis and interpretation of data (e.g., statistical analysis, biostatistics, computational analysis): L. Riolobos, P.M. Treuting, A.E. Timms, E.A. Hershberg, M.L. Disis
Writing, review, and/or revision of the manuscript: L. Riolobos, P.M. Treuting, E.A. Hershberg, L.R. Corulli, M.L. Disis
Study supervision: L. Riolobos, M.L. Disis

Acknowledgments

The authors wish to thank the staff of the University of Washington Comparative Pathology Program/Histology and Imaging Core Research Laboratory, especially Brian Johnson and Megan Larmore, for their contributions to slide production and histochemical staining. Thanks to Rebecca Hull-Meichle and Nishi Ivanov, from the University of Washington Diabetes Research Center, for the help with laser capture microdissection. We would also like to thank the staff at the NextGen Sequencing Core Facility at the Fred Hutchinson Cancer Research Center (FHCRC) for their support for the formalin-fixed, paraffin-embedded RNA sample preparation and RNA sequencing.

This work was supported by the NIH (HHSN261201200013I-HHSN26100009). M.L. Disis is supported by the Helen B. Slonaker Endowed Professor for Cancer Research and the American Cancer Society's Clinical Research Professor.

The costs of publication of this article were defrayed in part by the payment of page charges. This article must therefore be hereby marked *advertisement* in accordance with 18 U.S.C. Section 1734 solely to indicate this fact.

Received November 13, 2018; revised March 27, 2019; accepted May 14, 2019; published first May 17, 2019.

References

1. McFadden DG, Politi K, Bhutkar A, Chen FK, Song X, Pirun M, et al. Mutational landscape of EGFR-, MYC-, and Kras-driven genetically engineered mouse models of lung adenocarcinoma. Proc Natl Acad Sci U S A 2016;113:E6409–E17.
2. Busch SE, Hanke ML, Kargl J, Metz HE, MacPherson D, Houghton AM. Lung cancer subtypes generate unique immune responses. J Immunol 2016;197:4493–503.
3. Lu H, Knutson KL, Gad E, Disis ML. The tumor antigen repertoire identified in tumor-bearing neu transgenic mice predicts human tumor antigens. Cancer Res 2006;66:9754–61.
4. Wang Y, Rouggly L, You M, Lubet R. Animal models of lung cancer characterization and use for chemoprevention research. Prog Mol Biol Transl Sci 2012;105:211–26.
5. Wang Y, Zhang Z, Yan Y, Lemon WJ, LaRegina M, Morrison C, et al. A chemically induced model for squamous cell carcinoma of the lung in mice: histopathology and strain susceptibility. Cancer Res 2004;64:1647–54.
6. You MS, Rouggly LC, You M, Wang Y. Mouse models of lung squamous cell carcinomas. Cancer Metastasis Rev 2013;32:77–82.
7. Goodsell DS. The molecular perspective: nicotine and nitrosamines. Oncologist 2004;9:353–4.
8. Azpilikueta A, Agorreta J, Labiano S, Perez-Gracia JL, Sanchez-Paulete AR, Aznar MA, et al. Successful immunotherapy against a transplantable mouse squamous lung carcinoma with anti-PD-1 and anti-CD137 monoclonal antibodies. J Thorac Oncol 2016;11:524–36.

9. Xiong D, Pan J, Yin Y, Jiang H, Szabo E, Lubet RA, et al. Novel mutational landscapes and expression signatures of lung squamous cell carcinoma. Oncotarget 2018;9:7424–41.
10. Ambrosini V, Nanni C, Pettinato C, Fini M, D'Errico A, Trepidi S, et al. Assessment of a chemically induced model of lung squamous cell carcinoma in mice by 18F-FDG small-animal PET. Nucl Med Commun 2007;28:647–52.
11. Hudish TM, Opincariu LI, Mozer AB, Johnson MS, Cleaver TG, Malkoski SP, et al. N-nitroso-tris-chloroethylurea induces premalignant squamous dysplasia in mice. Cancer Prev Res 2012;5:283–9.
12. Dorak MT, Karpuzoglu E. Gender differences in cancer susceptibility: an inadequately addressed issue. Front Genet 2012;3:268.
13. Nikitin AY, Alcaraz A, Anver MR, Bronson RT, Cardiff RD, Dixon D, et al. Classification of proliferative pulmonary lesions of the mouse: recommendations of the mouse models of human cancers consortium. Cancer Res 2004;64:2307–16.
14. Renne R, Brix A, Harkema J, Herbert R, Kittel B, Lewis D, et al. Proliferative and nonproliferative lesions of the rat and mouse respiratory tract. Toxicol Pathol 2009;37:5S–73S.
15. Bankhead P, Loughrey MB, Fernandez JA, Dombrowski Y, McArt DG, Dunne PD, et al. QuPath: open source software for digital pathology image analysis. Sci Rep 2017;7:16878.
16. Disis ML, Gad E, Herendeen DR, Lai VP, Park KH, Cecil DL, et al. A multiantigen vaccine targeting neu, IGFBP-2, and IGF-IR prevents tumor progression in mice with preinvasive breast disease. Cancer Prev Res 2013;6:1273–82.
17. Park KH, Gad E, Goodell V, Dang Y, Wild T, Higgins D, et al. Insulin-like growth factor-binding protein-2 is a target for the immunomodulation of breast cancer. Cancer Res 2008;68:8400–9.
18. Love MI, Huber W, Anders S. Moderated estimation of fold change and dispersion for RNA-seq data with DESeq2. Genome Biol 2014;15:550.
19. Rehm S, Lijinsky W, Singh G, Katyal SL. Mouse bronchiolar cell carcinogenesis. Histologic characterization and expression of Clara cell antigen in lesions induced by N-nitrosobis-(2-chloroethyl) ureas. Am J Pathol 1991;139:413–22.
20. Puccini J, Dorstyn L, Kumar S. Genetic background and tumour susceptibility in mouse models. Cell Death Differ 2013;20:964.
21. Reilly KM. The effects of genetic background of mouse models of cancer: friend or foe? Cold Spring Harb Protoc 2016;2016:pdb top076273.
22. Klopstock N, Katzenellenbogen M, Pappo O, Sklair-Levy M, Olam D, Mizrahi L, et al. HCV tumor promoting effect is dependent on host genetic background. PLoS One 2009;4:e5025.
23. Ghosh M, Dwyer-Nield LD, Kwon JB, Barthel L, Janssen WJ, Merrick DT, et al. Tracheal dysplasia precedes bronchial dysplasia in mouse model of N-nitroso trischloroethylurea induced squamous cell lung cancer. PLoS One 2015;10:e0122823.
24. Cook MB, McGlynn KA, Devesa SS, Freedman ND, Anderson WF. Sex disparities in cancer mortality and survival. Cancer Epidemiol Biomarkers Prev 2011;20:1629–37.
25. Visbal AL, Williams BA, Nichols FC 3rd, Marks RS, Jett JR, Aubry MC, et al. Gender differences in non-small-cell lung cancer survival: an analysis of 4,618 patients diagnosed between 1997 and 2002. Ann Thorac Surg 2004;78:209–15; discussion 15.
26. Hsu LH, Chu NM, Liu CC, Tsai SY, You DL, Ko JS, et al. Sex-associated differences in non-small cell lung cancer in the new era: is gender an independent prognostic factor? Lung Cancer 2009;66:262–7.
27. Carey MA, Card JW, Voltz JW, Arbes SJ Jr, Germolec DR, Korach KS, et al. It's all about sex: gender, lung development and lung disease. Trends Endocrinol Metab 2007;18:308–13.
28. Forsslund H, Yang M, Mikko M, Karimi R, Nyren S, Engvall B, et al. Gender differences in the T-cell profiles of the airways in COPD patients associated with clinical phenotypes. Int J Chron Obstruct Pulmon Dis 2017;12:35–48.
29. Pinto JA, Vallejos CS, Raez LE, Mas LA, Ruiz R, Torres-Roman JS, et al. Gender and outcomes in non-small cell lung cancer: an old prognostic variable comes back for targeted therapy and immunotherapy? ESMO Open 2018;3:e000344.
30. Zang EA, Wynder EL. Differences in lung cancer risk between men and women: examination of the evidence. J Natl Cancer Inst 1996;88:183–92.
31. Lubin JH, Blot WJ. Assessment of lung cancer risk factors by histologic category. J Natl Cancer Inst 1984;73:383–9.
32. Risch HA, Howe GR, Jain M, Burch JD, Holowaty EJ, Miller AB. Are female smokers at higher risk for lung cancer than male smokers? A case-control analysis by histologic type. Am J Epidemiol 1993;138:281–93.
33. McDuffie HH, Klaassen DJ, Dosman JA. Female-male differences in patients with primary lung cancer. Cancer 1987;59:1825–30.
34. Kadel S, Ainsua-Enrich E, Hatipoglu I, Turner S, Singh S, Khan S, et al. A major population of functional KLRG1(-) ILC2s in female lungs contributes to a sex bias in ILC2 numbers. Immunohorizons 2018;2:74–86.
35. Polanczyk MJ, Hopke C, Vandenbark AA, Offner H. Estrogen-mediated immunomodulation involves reduced activation of effector T cells, potentiation of Treg cells, and enhanced expression of the PD-1 costimulatory pathway. J Neurosci Res 2006;84:370–8.
36. Polanczyk MJ, Hopke C, Vandenbark AA, Offner H. Treg suppressive activity involves estrogen-dependent expression of programmed death-1 (PD-1). Int Immunol 2007;19:337–43.
37. Schalper KA, Brown J, Carvajal-Hausdorf D, McLaughlin J, Velcheti V, Syrigos KN, et al. Objective measurement and clinical significance of TILs in non-small cell lung cancer. J Natl Cancer Inst 2015;107.
38. Al-Shibli KI, Donnem T, Al-Saad S, Persson M, Bremnes RM, Busund LT. Prognostic effect of epithelial and stromal lymphocyte infiltration in non-small cell lung cancer. Clin Cancer Res 2008;14:5220–7.
39. Munari E, Zamboni G, Lunardi G, Marchionni L, Marconi M, Sommaggio M, et al. PD-L1 expression heterogeneity in non-small cell lung cancer: defining criteria for harmonization between biopsy specimens and whole sections. J Thorac Oncol 2018;13:1113–20.